Microbial Alkalinity Production and Silicate Alteration in Methane Charged Marine Sediments: Implications for Porewater Chemistry and Diagenetic Carbonate Formation

Patrick Meister[1*], Gerhard Herda[1], Elena Petrishcheva[2], Susanne Gier[1*], Gerald R. Dickens[3], Christian Bauer[4], and Bo Liu[5]

[1] *Department of Geology, University of Vienna, Althanstr. 14, 1090 Vienna, Austria*
[2] *Department of Lithospheric Research, University of Vienna, Althanstr. 14, 1090 Vienna, Austria*
[3] *Department of Geology, Trinity College Dublin, 1 Park Lane East, Dublin 02, Ireland*
[4] *Institute of Mechanics and Mechatronics, Vienna University of Technology, Karlsplatz 13, 1040 Vienna, Austria*
[5] *Alfred-Wegener Institute, Helmholtz Centre for Polar and Marine Research, Am Handelshafen 12, 27570 Bremerhaven, Germany*

[*] *Corresponding authors:*
Patrick Meister: patrick.meister@univie.ac.at
Susanne Gier: susanne.gier@univie.ac.at

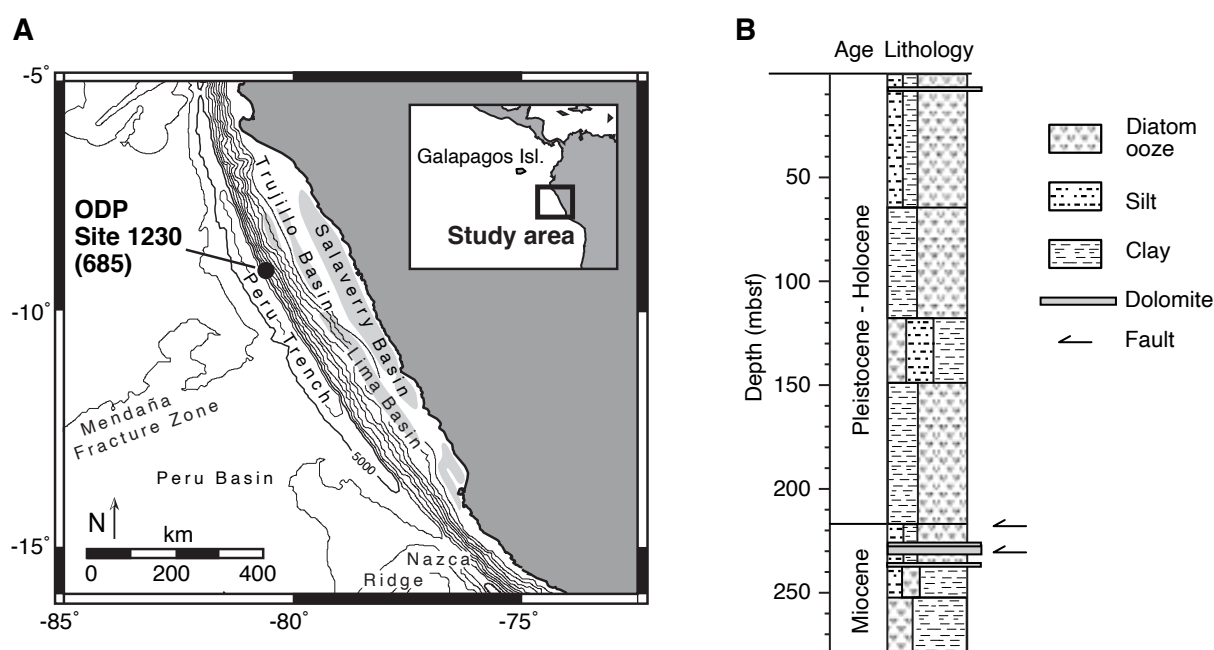## Supplement 1: Sampling site and lithology

FIGURE S1. (A) Map of the eastern Pacific/Peru margin showing the location of Ocean Drilling Program (ODP) Leg 201 Site 1230, which has been re-drilled at the same location as ODP Leg 112 Site 685. (B) Lithological column of the drilled sequence showing the main units and epochs. Modified from D'Hondt et al. (2003).

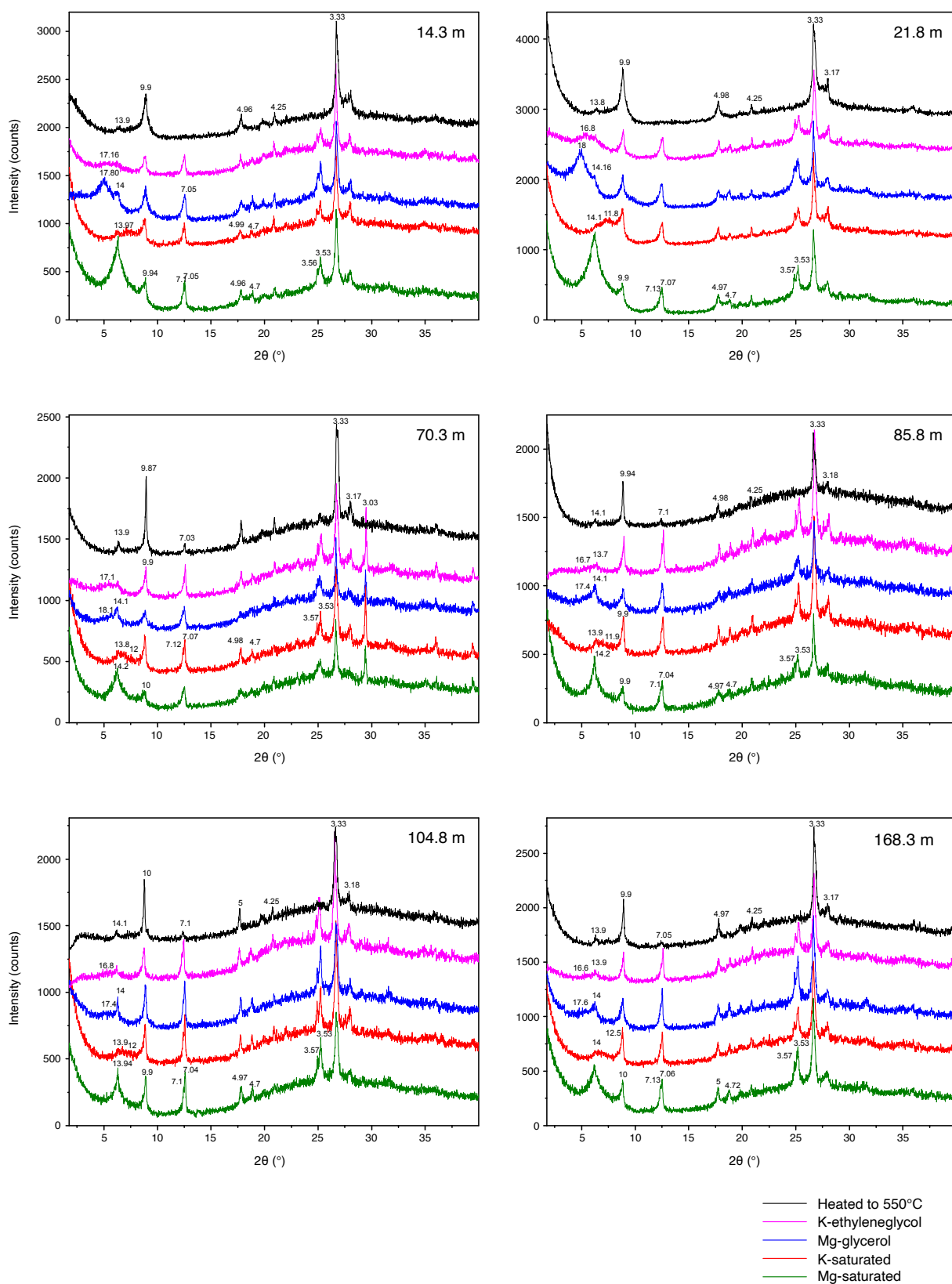# Supplement 2: XRD spectra of clay mineral separates

FIGURE S2. XRD spectra of clay mineral fractions: Mg-saturated, treated with glycerol, K-saturated, and treated with ethylene glycol, and fractions heated to 550°C.

Supplement 3: Sensitivity analysis of organic carbon degradation

Here provide additional parameter testing for the full-speciation reaction-transport model related to the degradation of organic matter. Organic carbon degradation is simulated by using the reactive-continuum model of Boudreau and Ruddick (1991).

$$TOC(t) = TOC_0 \left[\frac{a_{RC}}{(a_{RC} + t)} \right]^{\nu}$$

where $TOC(t)$ is the TOC at sediment age t, TOC_0 is the initial TOC upon sedimentation, and a_{RC} and ν are fitting parameters in the reactive continuum model. This model treats the complex mixture of potentially thousands of compounds as a reactive continuum, i.e. an infinite number of differently reactive compounds, where the distribution of reactivity constants is described by a distribution function (gamma function). The function has three variable parameters: TOC_0, a_{RC}, and ν.

   The parameters are constrained in the present model study by fitting the porewater profiles, in particular, the sulphate and methane profiles, as discussed in detail in Meister et al. (2013). A further constraint is given by the production of ammonium, which is linked to the TOC-degradation function via the C/N ratio. Both the C/N ratio and the compaction are well constrained using the measured data (see main text and Fig. 4).

Setting organic matter degradation parameters

To test the sensitivity of the model with respect to the three TOC degradation parameters, four different values of ν were chosen, which covers the range of realistic values (see Meister et al., 2013). For each ν the value of a was varied and TOC_0 was adjusted to fit the depth of the SMT to the measured data. The sensitivity analysis in Meister et al. (2013) has shown that an intermediate value for a results in the highest position of the SMT, while a large or small a would require larger TOC_0 to reach the SMT depth.

   The simulations (Fig. S1) show indeed that TOC_0 is smallest for intermediate values of a. For each ν, the cases labelled III are closest to the measured porewater data, and they show an increase in gas-hydrate-bound methane at the depth where the error bars are larger. It is generally observed that at high ν the alkalinity is somewhat too small at depth, whereas at small ν the ammonium curve shows too big of a "belly" at depth. The best compromise would be case III at ν = 0.3 (thick lines in panel B). In this case also the TOC curve is within the scatter of the data, while in the other cases, the TOC curve is far off.

   It is possible that variation of TOC induced non-steady state conditions. However, to resolve such variations the depositional history at Site 1230 is probably not sufficiently constrained.
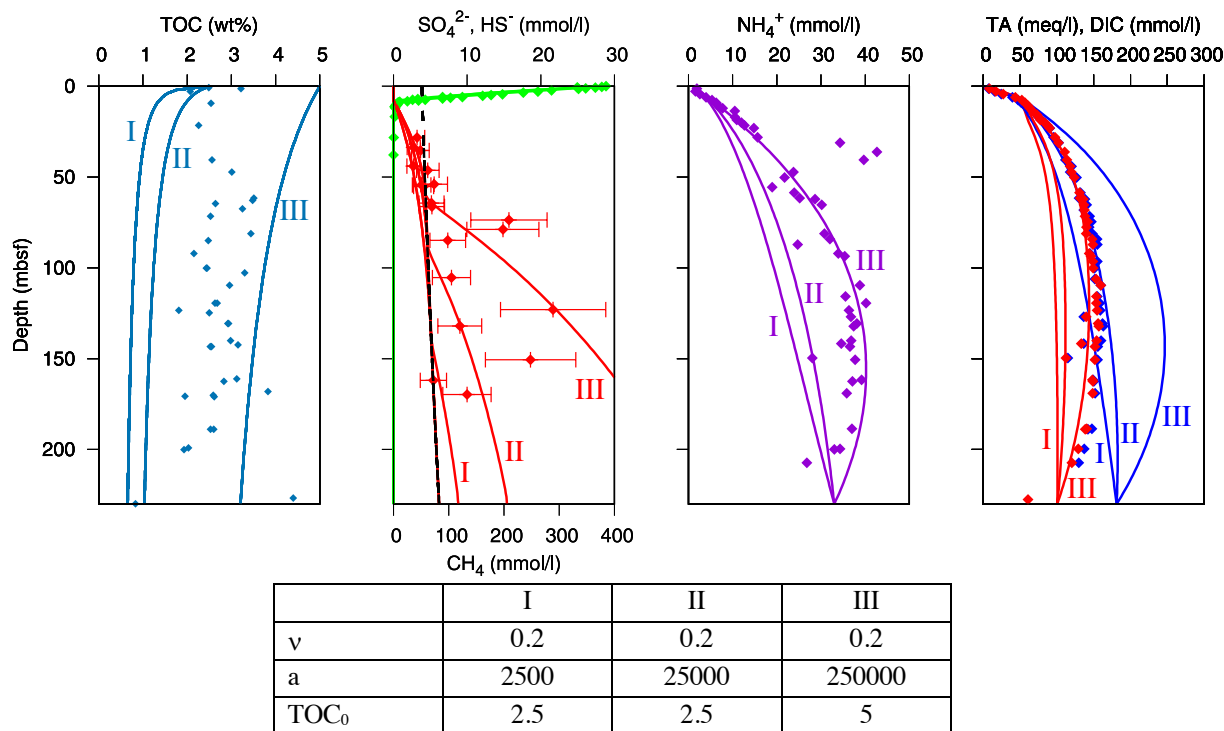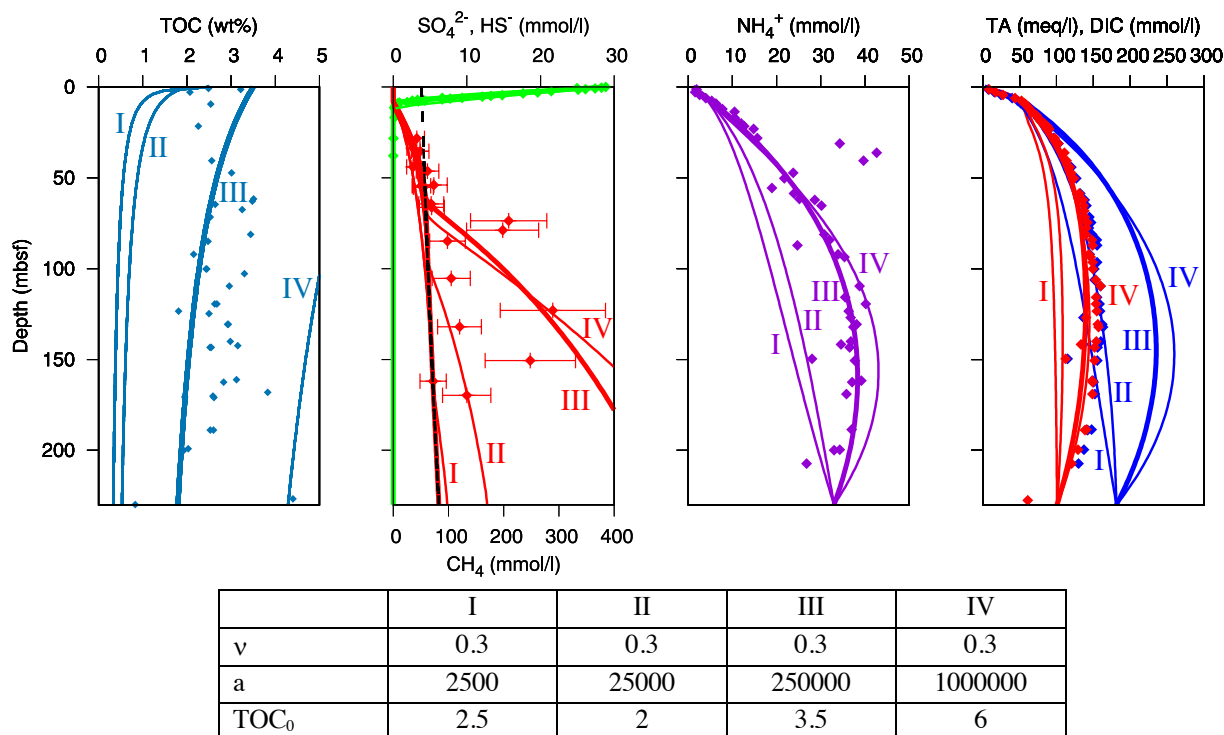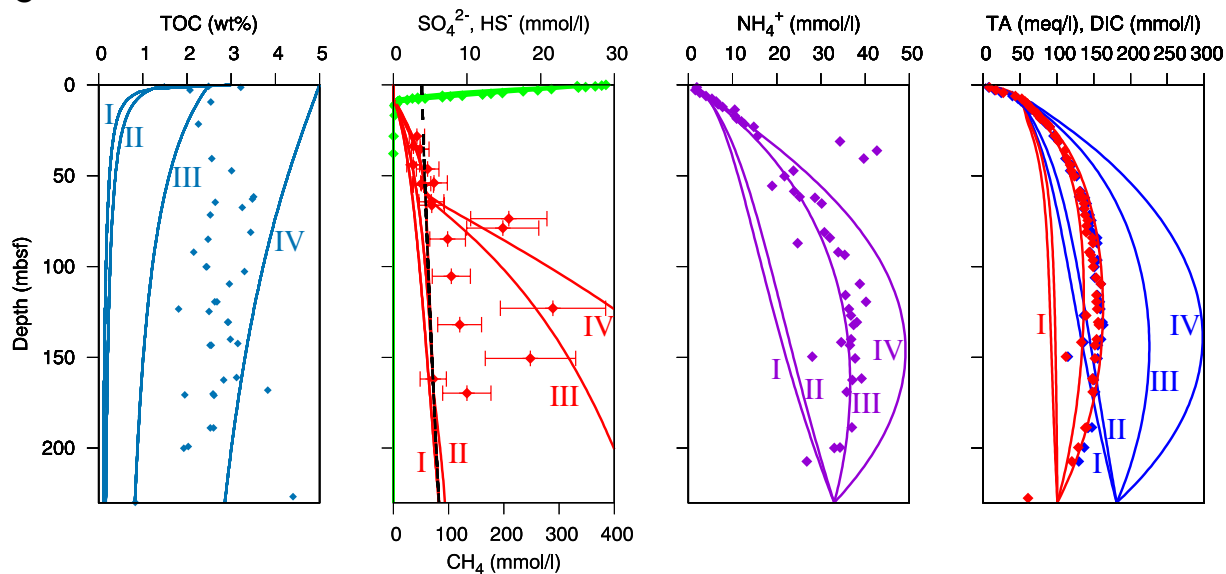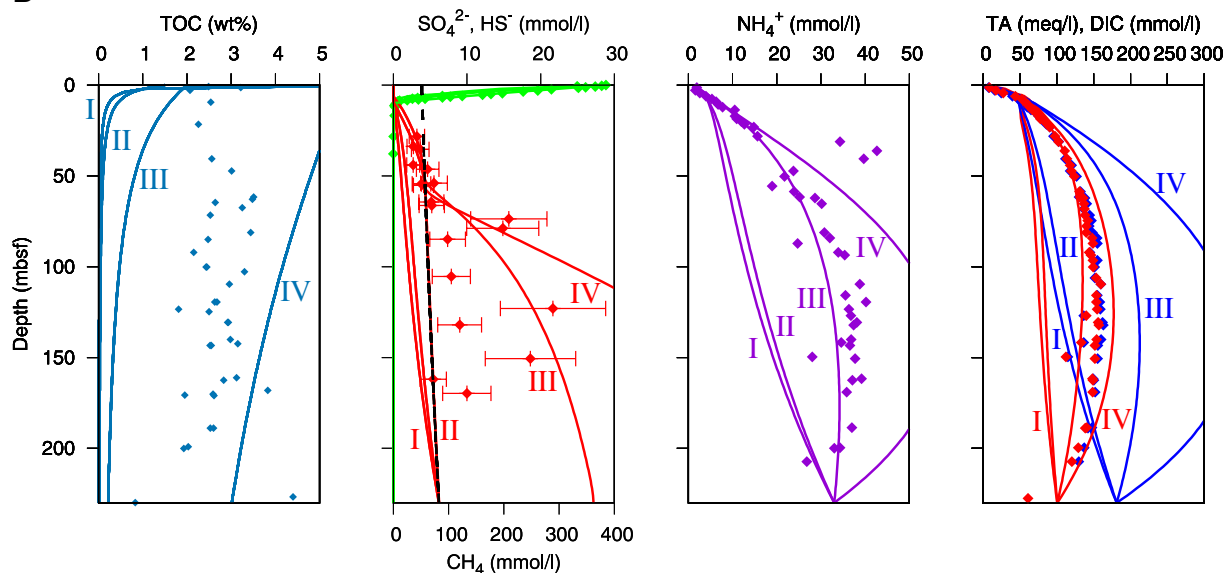
A

	I	II	III
ν	0.2	0.2	0.2
a	2500	25000	250000
TOC_0	2.5	2.5	5

B

	I	II	III	IV
ν	0.3	0.3	0.3	0.3
a	2500	25000	250000	1000000
TOC_0	2.5	2	3.5	6

FIGURE S3. Varying ν (0.2, 0.3, 0.5, 1, 2) at constant depth of the SMT. For each value of ν two different values for *a* are possible, so that the SMT is fitted. Data from D'Hondt et al. (2003) and Donohue et al. (2006).

C

	I	II	III	IV
ν	0.5	0.5	0.5	0.5
a	2500	25000	250000	1000000
TOC_0	3	1.5	2.5	5

D

	I	II	III	IV
ν	1	1	1	1
a	2500	25000	250000	2500000
TOC_0	6	1.5	2	5.5

FIGURE S3. Continued

5

Supplement 4: Sensitivity analysis of silicate reactions

We performed a more detailed analysis of the effect of the rate of silicate alteration on simulated porewater profiles. For silicate degradation an empirical function of the form:

$$k = k_\infty + (k_0 - k_\infty) \cdot e^{-(z/b)}$$

was fitted to the data. A constant rate constant k_{const} could not reproduce the mineral reactions to fit the measured porewater data. In particular, in the lower part of the model reaction rates slow down, which can already be observed qualitatively by the less curved porewater profiles in the lower part of the profiles. A decay of silicate reaction rates may have several reasons, such as decreasing accessibility due to compaction, reaction rim formation, or coating by secondary minerals.

Testing kinetic parameters

The kinetic rate law shown above can be fitted by varying three different parameters: k_∞ is the rate constant at infinite depth, which can be set to zero. Any value large than zero would increase the bulge, in particular of the Mg-profile near the base. The variable parameters are then k_0 (k at the surface) and the decay constant b.

In the test series shown in Fig. S4 three different values for the decay constant b were selected that are both smaller and larger than the best fit (10, 20, and 50). For each value of b, k_0 was then varied over a range encompassing the best fit.

The resulting reaction rate is a result of the downward decreasing k and the saturation state (see Fig. 6 in main text). As for several clay minerals, including vermiculite, the SI reaches a maximum at the SMT and then decreases with depth, an s-shape curvature is seen in the downward simulation of the reaction rate. The best fit is reached for a decay constant of 20, in which case the bulge in the Mg and K profiles are at the right depth. The best fit can then be found for $k_0 = 0.00005$ (thick line in panel B). A slight curvature of the Mg-profile in the lower part of the profile is due to the effect of downward burial and cannot be avoided.
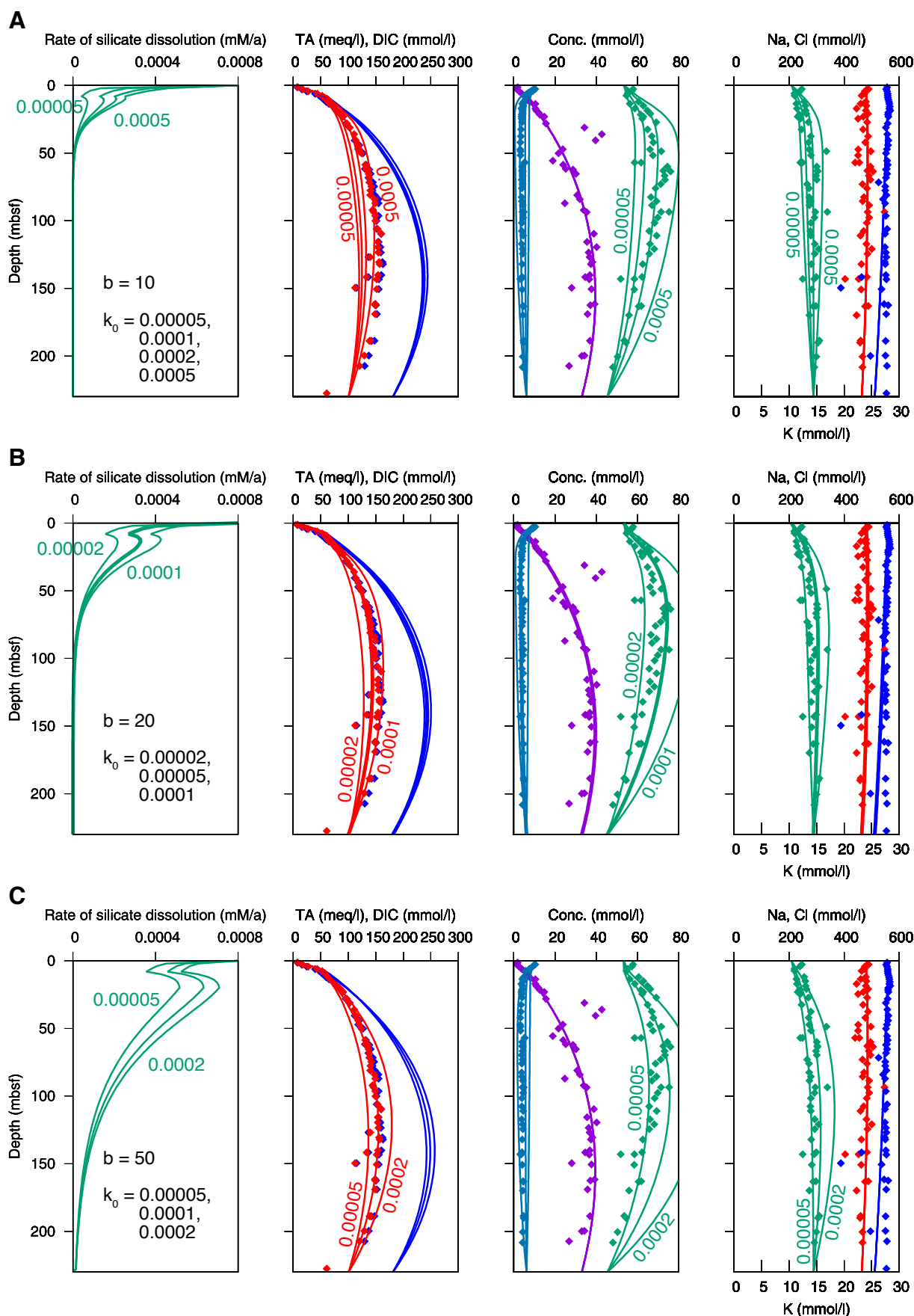
FIGURE S4. Testing kinetic parameters for K-vermiculite degradation, using the values: (A) b 10, (B) 20, and (C) 50. k_∞ was set as zero and k_0 was varied from 0.00002 to 0.0005. Data are from D'Hondt et al. (2003) and Donohue et al. (2006).

7

Testing other clay minerals

X-ray diffraction has provided evidence for the presence of a range of different clay minerals: smectite, illite, kaolinite, chlorite, and vermiculite. Furthermore, also K-feldspar and albite are present. The large contribution of opal A is based on sedimentological observation, whereby the incipient ripening to opal C/T is evident based on the hump in the baseline of the diffractograms.

While kaolinite is the only silicate mineral that is clearly supersaturated, it is most likely linked to the dissolution of undersaturated silicates via the insoluble aluminium. At the same time, the silica content is buffered by opal C/T precipitation (see main text for details).

In this case, the variable mineral reactions would be with smectite, illite, chlorite, vermiculite, K-feldspar, and albite. Out of these, only chlorite and vermiculite are significantly undersaturated while the other ones are near to saturation. In this test we demonstrate that including all of these silicates using the same degradation parameters as constrained above for vermiculite would result in an insignificant deviation from the profiles used with just vermiculite in it (Fig. S5A). In other words, the other silicates can be essentially ignored, except chlorite.
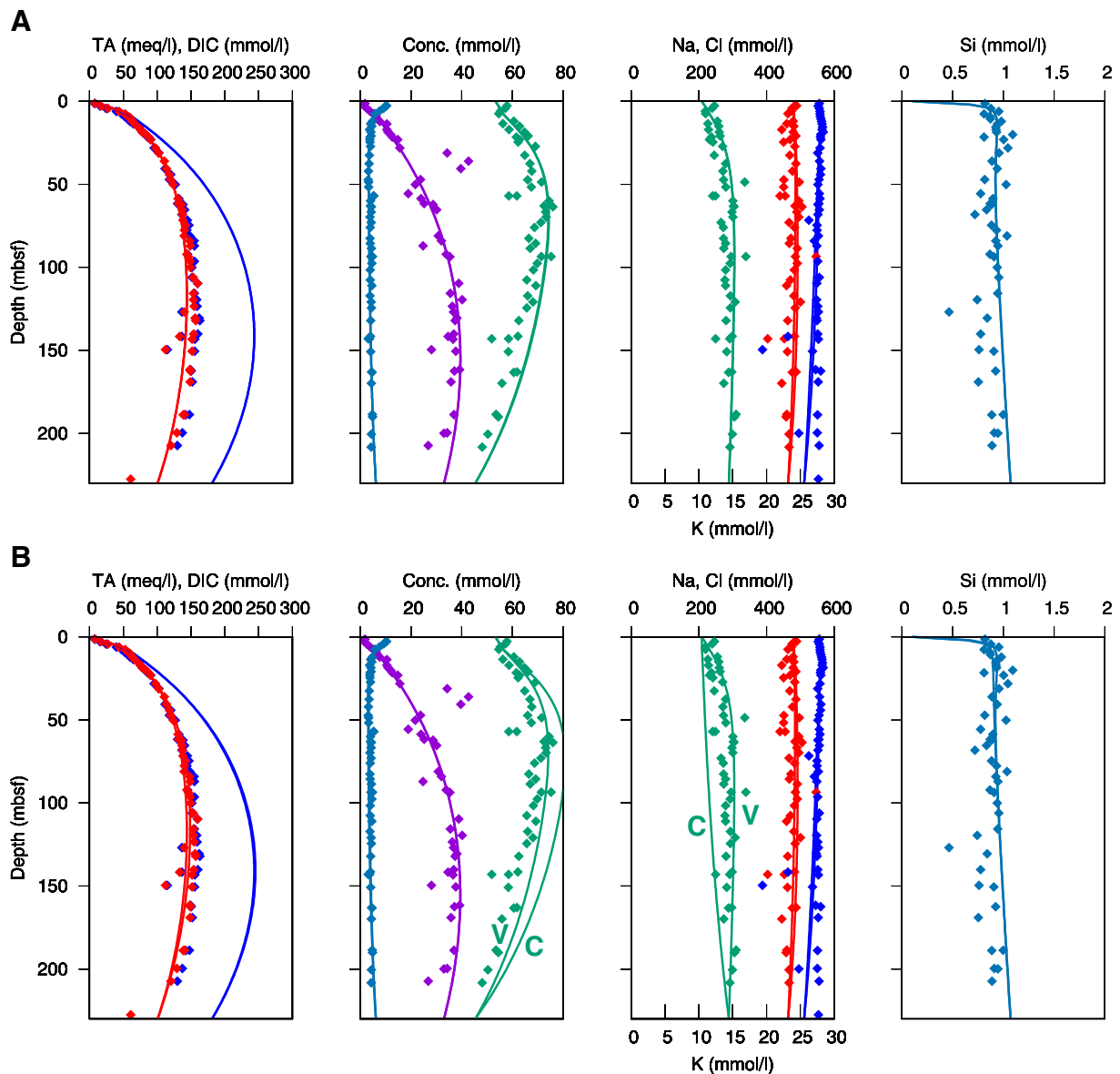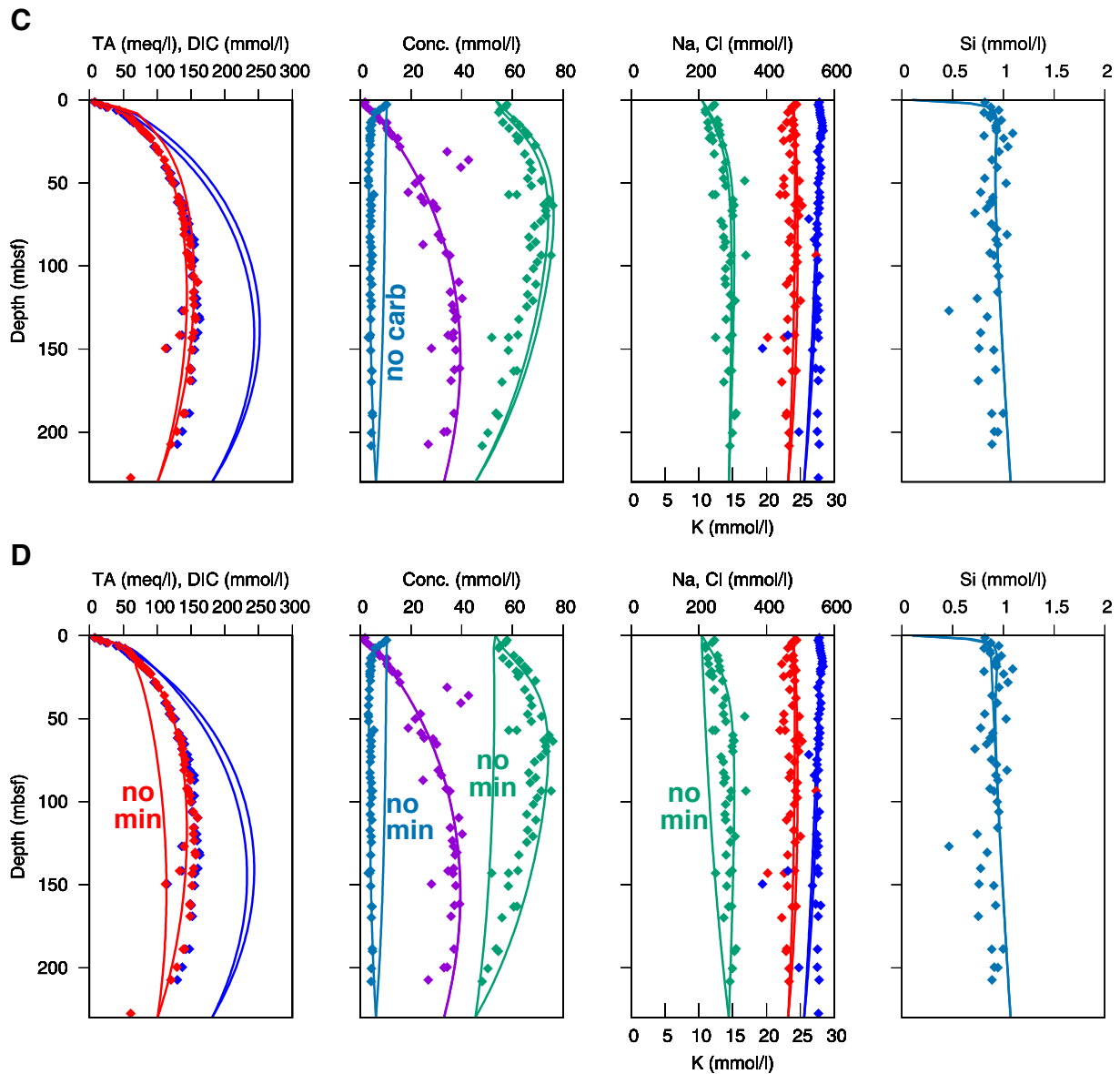
FIGURE S5. Model results showing the effects of different mineral reactions. (A) Simulation including reaction with all minerals except chlorite, using the rate constant function of vermiculite (best fit in Fig. S4B) in comparison with using only vermiculite. (B) Comparison of cases with reaction of chlorite vs. vermiculite (including reactions of kaolinite and opal). (C) Simulations with and without carbonate (dolomite) precipitation. (D) Simulations with and without mineral reactions (except reactions with opal). Data are from D'Hondt et al. (2003) and Donohue et al. (2006).

The reactions of chlorite and vermiculite can well explain the source of Mg, however, the only potential source for K would be vermiculite. Panel B in Fig. S5 shows the difference between the two cases in with chlorite or vermiculite is reacted. Only with vermiculite, that observed K profile can be reproduced. As mentioned, illite is not sufficiently undersaturated to serve as a significant source of K. The only alternative source of K in porewater would be dissolution of volcanic ash, which we can neither confirm nor exclude for this site.

In order to demonstrate the overall effect of mineral reactions, we display the results with no carbonate precipitation in panel C (Fig. S5). This shows that the shape of the Ca curve is clearly reproduced by a focused precipitation of carbonate near the SMT, due to the maximum in supersaturation.

Furthermore, panel D shows the comparison of the best fit with no mineral reactions (except buffering of silica by opal C/T formation. In this case, Ca, Mg, and K just show the diffusive gradient imposed by the different upper and lower boundary conditions.

Conclusions on mineral reactions

In conclusion, clay mineral reactions are controlled either by K-rich vermiculite or chlorite in combination with an unknown source of K and concomitant precipitation of kaolinite due to coupling by Al. This reaction corresponds to a degradation of clay minerals commonly described, where cation oxides are going to solution, producing additional alkalinity in the porewater. The excess silica is then buffered by opal diagenesis.

References

Boudreau, B. P., and Ruddick, B. R. (1991). On a reactive continuum representation of organic matter diagenesis. American J. of Science 291, 507–538.

D'Hondt, S. L., Jørgensen, B. B., Miller, D. J., and the Shipboard Scientific Party (2003). Proc. ODP, Init. Repts. 201, Ocean Drilling Program, Texas A&M University, College Station TX 77845-9547, USA.

Donohue, C. M., Snyder, G. T., and Dickens, G. R. (2006). "Data report: Major cation concentrations of interstitial waters collected from deep sediments of Eastern Equatorial Pacific and Peru Margin (ODP Leg 201)," in eds B. B. Jørgensen et al., Proc. ODP, Sci. Results 201, 1–19, Ocean Drilling Program, College Station, Texas. doi:10.2973/odp.proc.sr.201.104.2006

Meister, P., Liu, B., Ferdelman, T. G., Jørgensen, B. B., and Khalili, A. (2013). Control of sulphate and methane distributions in marine sediments by organic matter reactivity. Geochim. Cosmochim. Acta. 104, 183–193.